Journal of Sound and Vibration (1998) **212**(3), 511–523

ACTIVE NOISE CONTROL OF ACOUSTIC SOURCES USING SPHERICAL HARMONICS EXPANSION AND A GENETIC ALGORITHM: SIMULATION AND EXPERIMENT

T. Martin and A. Roure

Laboratoire de Mécanique et d'Acoustique, 31 *chemin Joseph Aiguier*, 13402 *Marseille Cedex* 20, *France*

(*Received* 9 *January* 1997, *and in final form* 27 *November* 1997)

A general method is presented to optimize transducer location in an active noise control problem. The method includes two parts. First, the actuator configuration is determined by using a model of the primary field which is a spherical harmonics expansion. In the second part, a genetic algorithm is used to determine the error sensor configuration. This method is then applied to two real acoustic sources: a dipole and an electrical transformer. In numerical simulations, the primary field of both sources measured in an anechoic room was used to determine the active control configurations. Then, the actuator and error sensor arrangement was tested in an active control experiment involving both primary sources.

1. INTRODUCTION

In a first paper [1], it was shown that the actuators for the active noise control of a sound source radiating in free field could be determined through a model of the primary field. Spherical harmonics expansion and the correspondence between the series terms and multipolar sources make it possible to estimate the number and the arrangement of actuators to minimize the primary field. These actuators are located around points shifted from the primary source and called acoustical centres. Numerical simulations gave the optimal number and positions of the acoustical centres and the number of actuators per centre for classical primary sources (monopole, dipole).

The aim of the present paper was to evaluate the efficiency of the method on real noise sources whose sound field is measured in an anechoic room. The first source studied was a dipole made of two small loudspeakers; the second was an industrial electrical transformer. The location of a restricted number of error sensors was then optimized by using a genetic algorithm. The practical and realistic configurations of actuators and error sensors established from numerical simulations were then experimentally tested in real time. Finally, the numerical and experimental results of the active noise control of both primary sources is compared.

2. DIPOLAR PRIMARY SOURCE

2.1. DESCRIPTION OF THE EXPERIMENT

Figure 1 describes the experimental set-up. The primary dipole oriented in the (Ox) direction is located at the origin of a hemispherical antenna with a 3m radius. The

0022–460X/98/180511 + 13 $25.00/0/sv971444

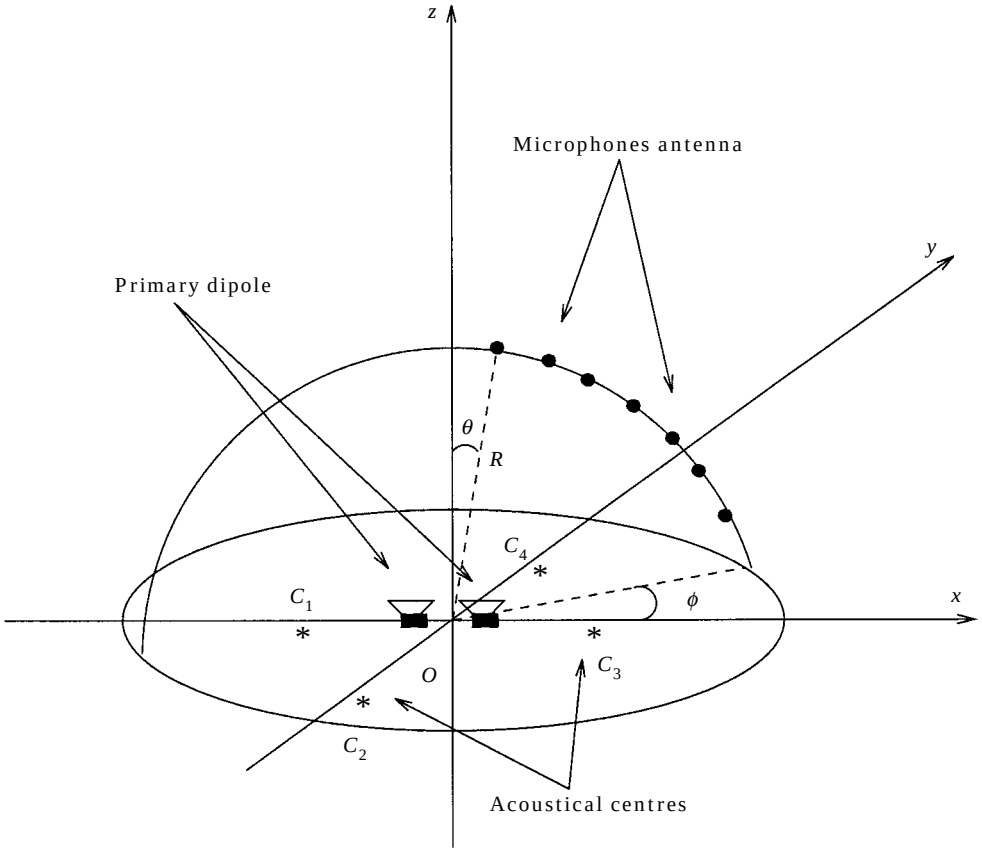

Figure 1. Geometrical description of the experiment.

acoustical centres C_j for the spherical harmonics expansion are located around the primary source. The rotation of the antenna of seven microphones gives 30 positions in azimuth, hence 210 measurement points M_i all around the primary source.

2.2. ACTUATOR CONFIGURATION

The actuator arrangement is determined by minimizing the functional

$$J = \sum_{i=1}^{210} |P(M_i) - \tilde{P}(M_i)|^2, \tag{1}$$

TABLE 1

Primary dipole, $f = 100$ Hz, *two acoustical centres at* $x = \pm 1$ m

Series coefficient	Acoustical centres positions	
	$x = -1$	$x = 1$
$\|A_{00}\|$	0·31	0·31
$\|A_{10}\|$	0·01	0·01
$\|A_{11}\|$	0·30	0·30
$\|B_{11}\|$	0·00	0·00

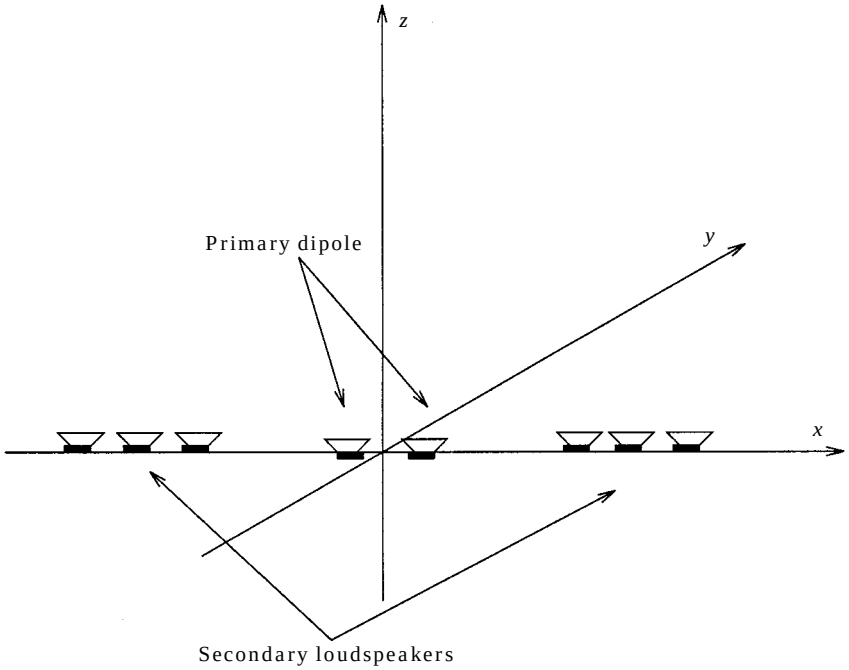

Figure 2. Actuators arrangement for the primary dipole.

where $\tilde{P}(M_i)$ is the pressure measured on point M_i and $P(M_i)$ is the model of the primary field,

$$P(M_i) = \sum_{j=1}^{n_c} \left[\sum_{n=0}^{N_j} h_n(kR_{ij}) \sum_{m=0}^{n} A_{nm}^j P_n^m(\cos\theta_{ij}) \cos m\phi_{ij} + \sum_{n=1}^{N_j} h_n(kR_{ij}) \sum_{m=1}^{n} B_{nm}^j P_n^m(\cos\theta_{ij}) \sin m\phi_{ij} \right], \quad (2)$$

where n_c is the number of acoustical centres C_j and $(R_{ij}, \theta_{ij}, \phi_{ij})$ are the co-ordinates of each point M_i in the co-ordinate system centred at C_j.

The model $P(M_i)$ is a series of spherical harmonics functions. Each model parameter A_{nm}^i and B_{nm}^j deduced from equation (1) corresponds to a multipolar source, and the association of all these sources gives the actuator arrangement (see reference [1] for further details). The coefficient A_{00} corresponds to a monopolar secondary source, and the coefficients A_{10}, A_{11} and B_{11} correspond to three dipolar secondary sources oriented in the directions (Oz), (Ox) and (Oy). The coefficients of order two correspond to quadripolar sources and so on.

In reference [1], we numerically evidenced the influence of the distance between the primary source and the secondary sources located around one or more acoustical centres. We also showed that it was of interest to use spherical harmonics expansion truncated at

1	0	1	1	0	0	0	1	0	1

Figure 3. Selection of five error sensors among 10.

TABLE 2

Global reduction GR (dB) *for six secondary loudspeakers and* 210 *or seven error microphones*

Number of		Frequency (Hz)		
Loudspeakers	Error microphones	100	200	300
6	210	17·4	16·4	12·0
6	7	15·6	16·2	10·4

order 1 for two acoustical centres arranged symmetrically with respect to the primary dipole on its directivity axis. Table 1 gives the results obtained when the field radiated by the dipole is measured experimentally. Only the A_{00} and A_{11} terms are identified; this corresponds to two groups of three actuators aligned on the (Ox) axis and located at 1 m from the primary dipole (cf. Figure 2).

2.3. ERROR SENSOR CONFIGURATION

At this point, the active noise control system is composed of six secondary loudspeakers as in Figure 2, and 210 error sensors located at the antenna points. A genetic algorithm was used to reduce the number of error sensors and to optimize their locations.

2.3.1. *Genetic algorithm*

The choice of a genetic algorithm was imposed because of the characteristics of the problem. The aim is to select seven error microphone positions among 210 to keep a

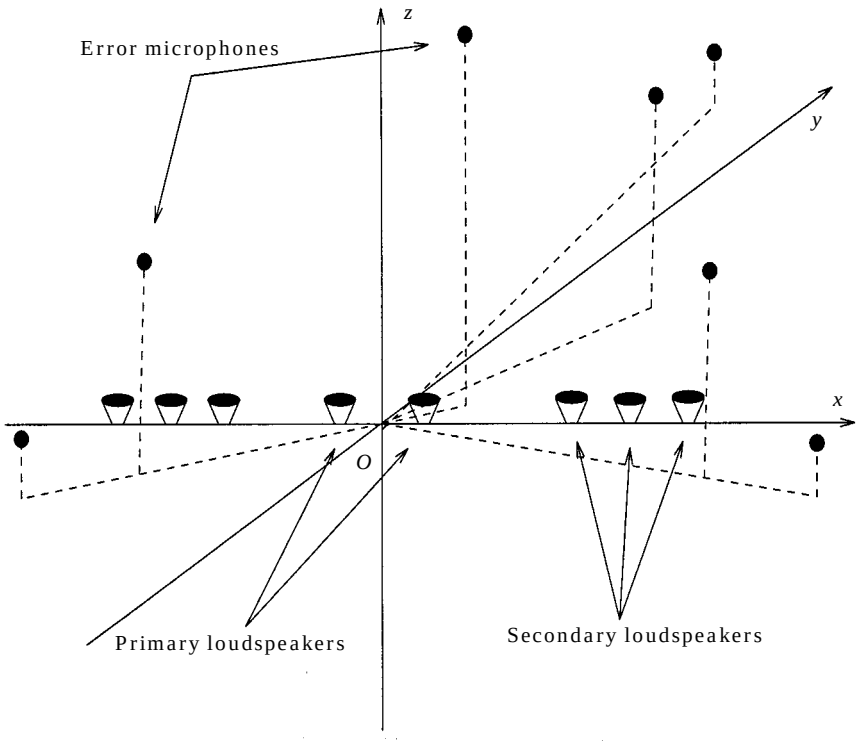

Figure 4. Geometrical arrangement of the active control system.

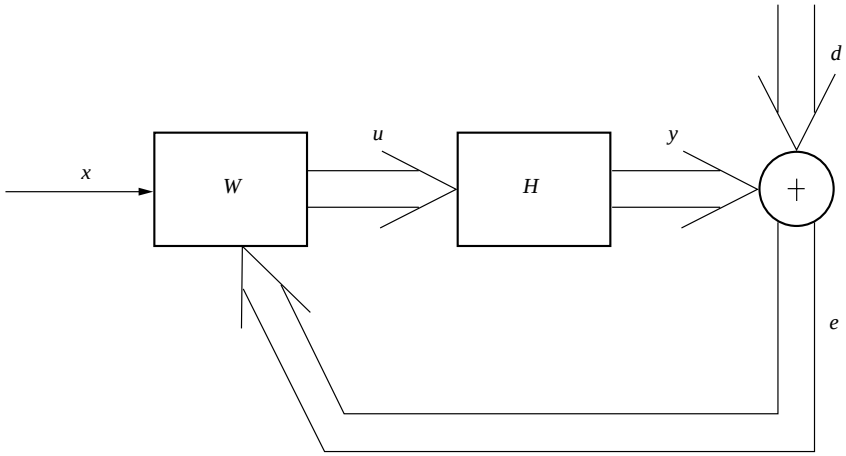

Figure 5. Block diagram of the X-LMS feedforward algorithm.

number of sensors slightly greater than the number of actuators. This is a selective search problem which is non-convex with a large degree of freedom. The genetic algorithm allows one to approach the optimal solution in a relatively short computation time. Another important feature of the algorithm is that it gives a set of "good" solutions which allows one to select the easiest one to implement for the experiment.

The genetic algorithms are described in references [2–4]. Briefly, the first step is to use a binary coding of the problem; this consists of strings called chromosomes corresponding to error sensor configurations and containing 1 and 0. Each element of the string corresponds to a sensor position; the value 1 indicates that the sensor is selected (Figure 3). In our case, the number of 1s per chromosome was 7 and the length of each chromosome was 210. We randomly generated a set of chromosomes called the initial generation. We evaluated the efficiency of each configuration of error sensors by using the following fitness function:

$$GR(f) = 10 \log \frac{\sum_{i=1}^{210} |P_p(M_i)|^2 \Delta S_i}{\sum_{i=1}^{210} |P_r(M_i)|^2 \Delta S_i}, \tag{3}$$

where $P_p(M_i)$ is the measured primary sound pressure at point M_i for frequency f, $P_s(M_i)$ is the secondary sound pressure computed for the configuration selected by the algorithm, $P_r(M_i) = P_p(M_i) + P_s(M_i)$ is the residual sound pressure and ΔS_i is the surface element associated with point M_i. We used the three basic genetic operators (reproduction,

TABLE 3

Global reduction GR (dB) *for the active control configuration of Figure* 4

	Frequency (Hz)		
GR (dB)	100	200	300
Numerical	15·6	16·2	10·4
Experimental	11·3	16·6	10·1

cross-over and mutation) and an elitist model which keeps the best chromosome for each generation. The number of chromosomes per generation was 20, the number of generations tested (number of iterations of the algorithm) was 200, the cross-over probability was 0·6, and the mutation probability was 0·1.

2.3.2. *Results*

The algorithm was run for $f = 200$ Hz, and the most efficient configurations were kept. Among them, the configuration giving the best results at 100 and 300 Hz was selected. Table 2 compares the results obtained with the seven error microphones selected by the algorithm and those obtained with the 210 error microphones at the beginning. The reduction obtained with seven microphones was equivalent to that with 210 microphones. The best adequacy was obtained at 200 Hz because the genetic algorithm was run at this frequency. The results obtained with these seven error microphones were compared with the results obtained with seven error microphones uniformly distributed around the

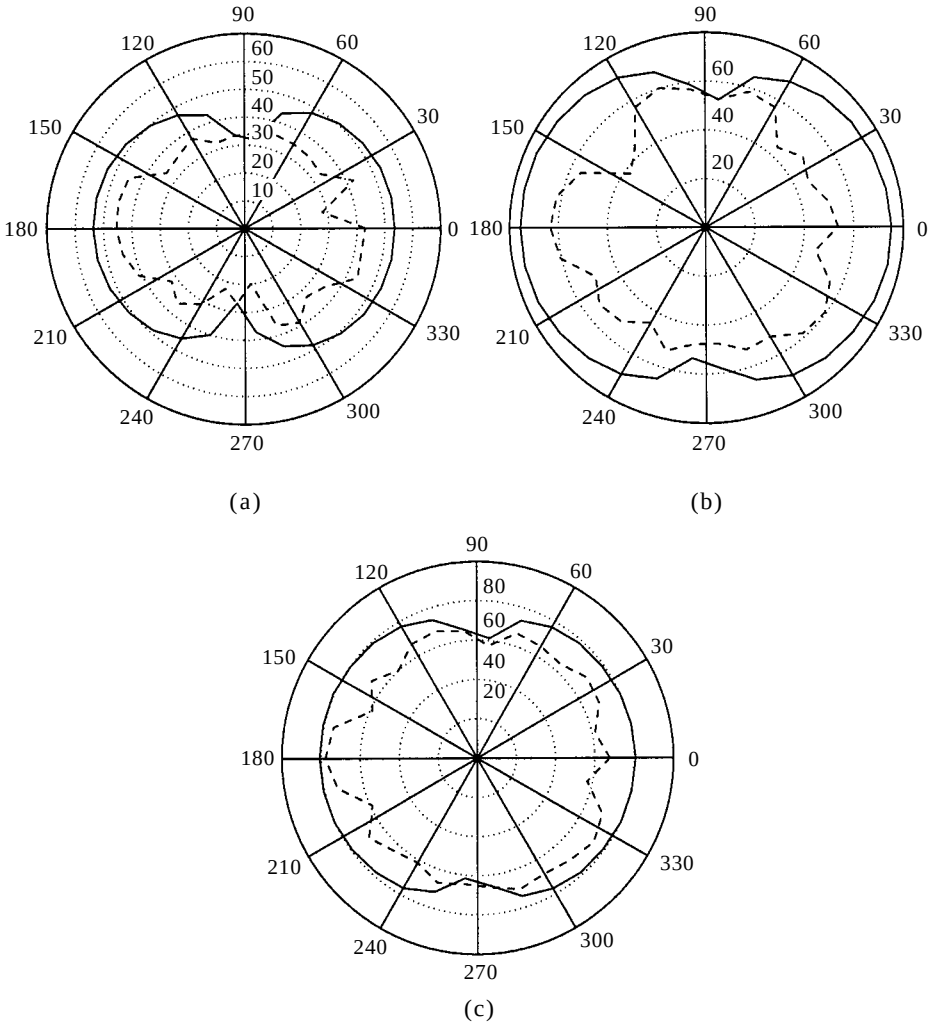

Figure 6. Sound pressure levels (dB) in the ($\theta = 13\pi/30$) plane, without control (——), with control (—), for the active control system of Figure 4: (a) 100 Hz; (b) 200 Hz; (c) 300 Hz.

primary source at positions $\phi = 0$, $2\pi/3$, $4\pi/3$ in the $\theta = 13\pi/30$ plane, $\phi = \pi/3$, π, $5\pi/3$ in the $\theta = 7\pi/30$ plane, and $\phi = 0$ in the $\theta = \pi/30$ plane. Only 6, 10 and 2 dB were obtained at 100, 200 and 300 Hz with this configuration, which is less than the reduction obtained with the genetic algorithm configuration. This justifies the use of the genetic algorithm and its optimization role.

2.4. ACTIVE CONTROL EXPERIMENT

The configuration of actuators and error sensors were implemented in the anechoic room to reduce the sound pressure radiated by the primary dipole. Figure 4 describes the geometrical arrangement of the control system in space. Small cubic loudspeakers were used of size (10 cm) and power (30 W), electret microphones and an electronic controller (10 inputs, 8 outputs) composed of a TMS320C25 DSP. A standard X-LMS feedforward algorithm (cf. Figure 5) was used with off-line secondary path identification and

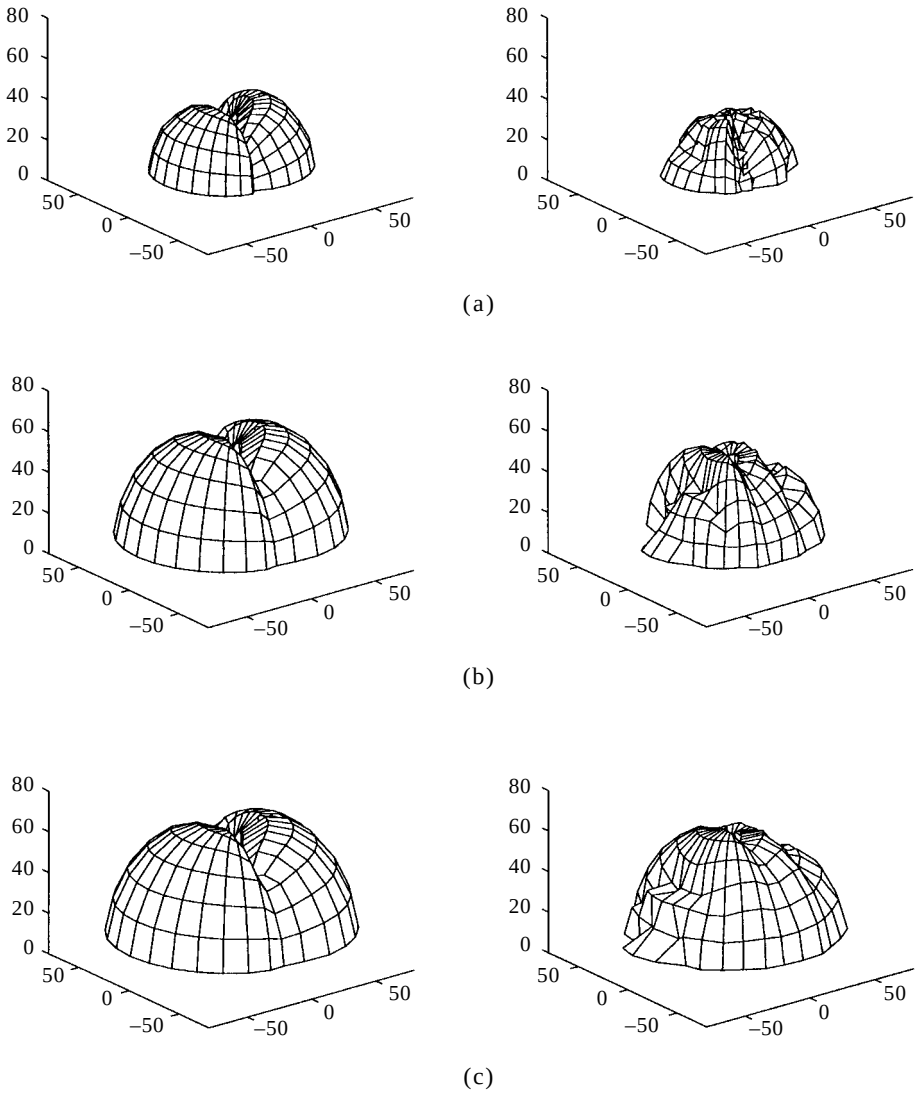

Figure 7. Sound pressure levels (dB) on the 210 antenna points, without control (left), with control (right), for the active control system of Figure 4: (a) 100 Hz; (b) 200 Hz; (c) 300 Hz.

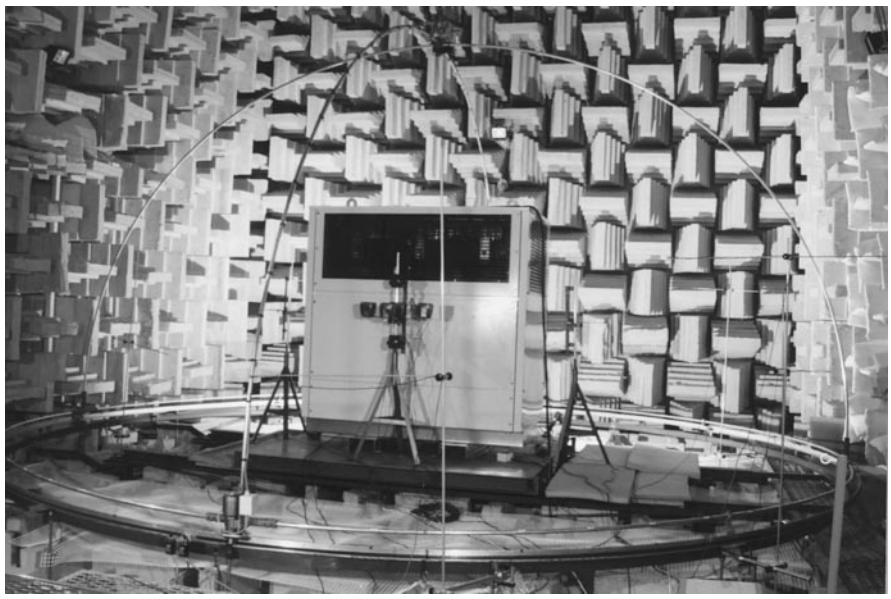

Figure 8. Transformer and measurement antenna.

the following parameters: sampling frequency $F_e = 1500$ Hz; cut-off frequency of the anti-aliasing filters $F_c = 630$ Hz; length of the filters corresponding to the impulse responses $N_h = 12$; length of the adaptive filters $N_w = 12$. The reference was an electrical signal composed of sine waves feeding the primary loudspeakers and taken from a generator. The convergence factor of the algorithm was chosen in order to obtain

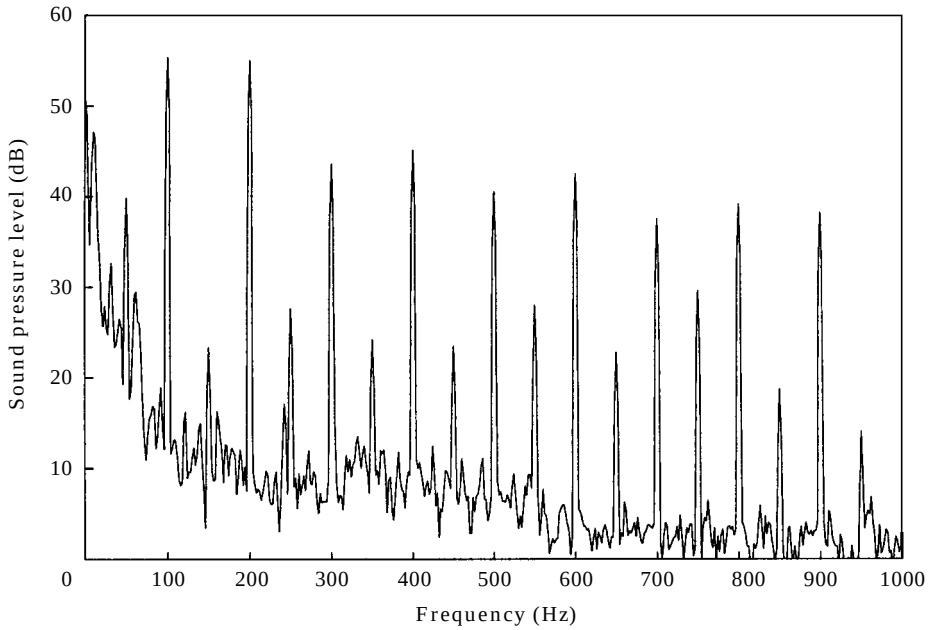

Figure 9. Transformer sound spectrum.

convergence in a few seconds and a good stability. A reduction from 20 to 30 dB was obtained on error microphones. The sound pressure level with and without active control was measured on the 210 measurement points of the hemispherical antenna. Table 3 compares the experimental results with the numerical ones of Table 2. Figures 6 and 7 show the experimental sound pressure levels, with and without control, measured on the 30 points in the lower plane of microphones ($\theta = 13\pi/30$) and on the 210 antenna points.

Table 3 shows that the numerical and experimental values of the reduction are equivalent. This reduction is an approximation of the sound power reduction; thus, the total sound power radiated by the primary dipole is reduced. Figures 6 and 7 show that the sound pressure level of the primary source is reduced in all directions and that the reduction also occurred in directions where there were no error sensors. A microphone located at 8 m from the primary source and $z = 1{\cdot}8$ m also gave a significant reduction of sound pressure. It is therefore possible to reduce in the whole space the sound emitted from a very directive primary source like a dipole with only six secondary loudspeakers and seven error microphones. Similar results were obtained with a monopolar primary source. Thus, the optimization method using spherical harmonics expansions and the genetic algorithm is very efficient for primary sources of small dimensions and leads to a practical and very simple system of active control.

3. EXTENDED PRIMARY SOURCE: ELECTRICAL TRANSFORMER

To evaluate the efficiency of the mixed method based on spherical harmonics expansion and genetic algorithm in the case of a more complicated and extended primary source, an

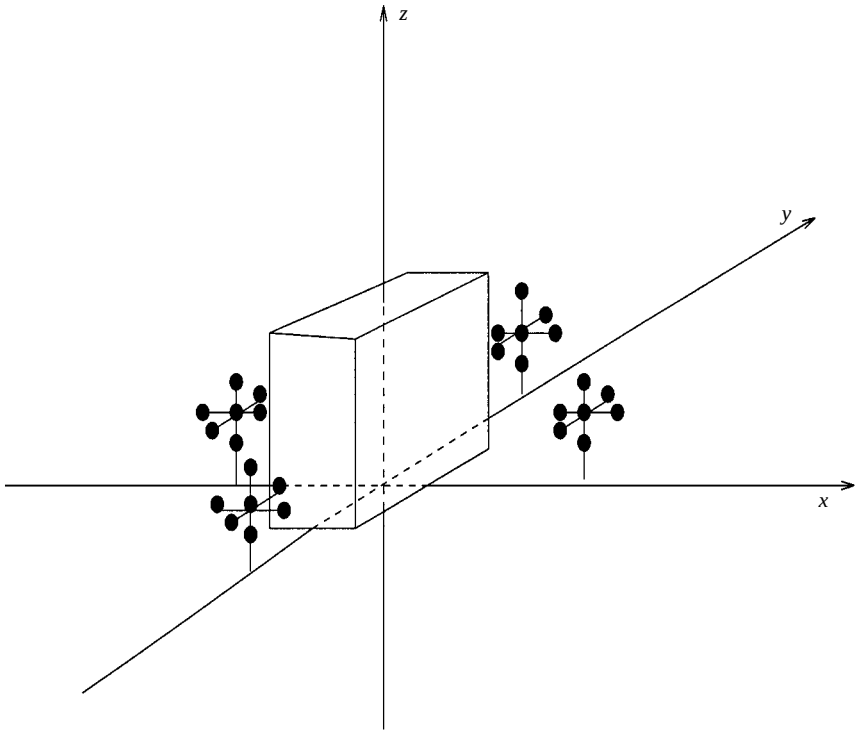

Figure 10. Actuators configuration for the transformer.

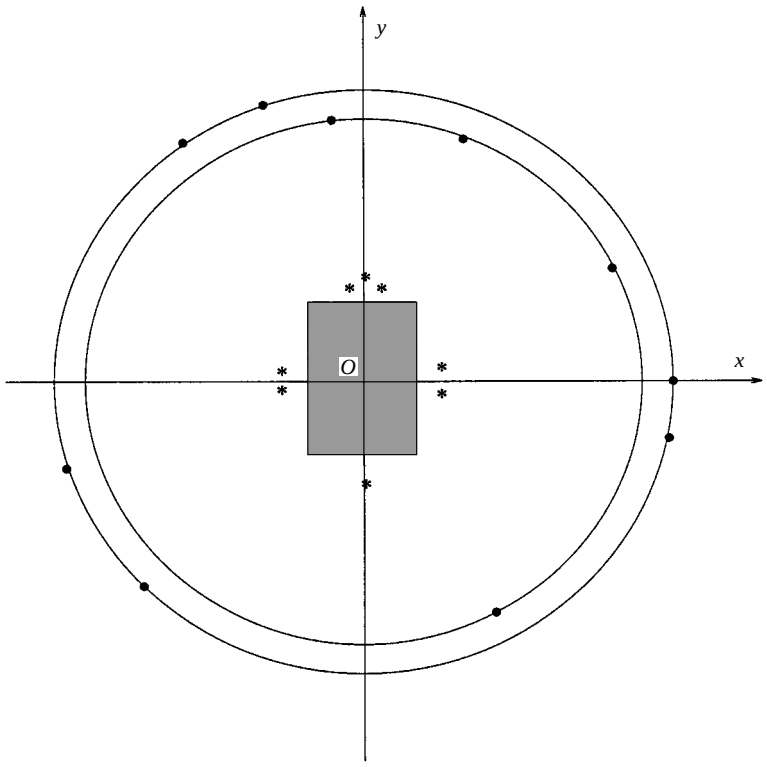

Figure 11. Active control system for the transformer: secondary loudspeakers (*), error microphones (●).

industrial electric transformer was used: voltage 20 kV/410 V; power 630 kVA; dimensions $L = 163$ cm, $l = 95$ cm, $H = 180$ cm; weight 2000 kg.

3.1. DESCRIPTION OF THE TRANSFORMER

Figure 8 shows the transformer and the antenna in the anechoic room. Figure 9 is the sound spectrum of the transformer.

3.2. ACTUATOR CONFIGURATION

Spherical harmonics expansions truncated at order 1 were used and a configuration of actuators was chosen with four acoustical centres symmetrically arranged around the transformer at a distance of 1 m. The number of secondary loudspeakers per centre was seven so the total number of actuators was 28 (Figure 10). Although this configuration was realistic and feasible, it was decided to decrease the number of loudspeakers to obtain a very simple active control system for the experiment.

TABLE 4

GR (dB) *for the active control configuration of Figure* 11

	Frequency (Hz)	
GR (dB)	100	200
Numerical	13·8	6·8
Experimental	11	5

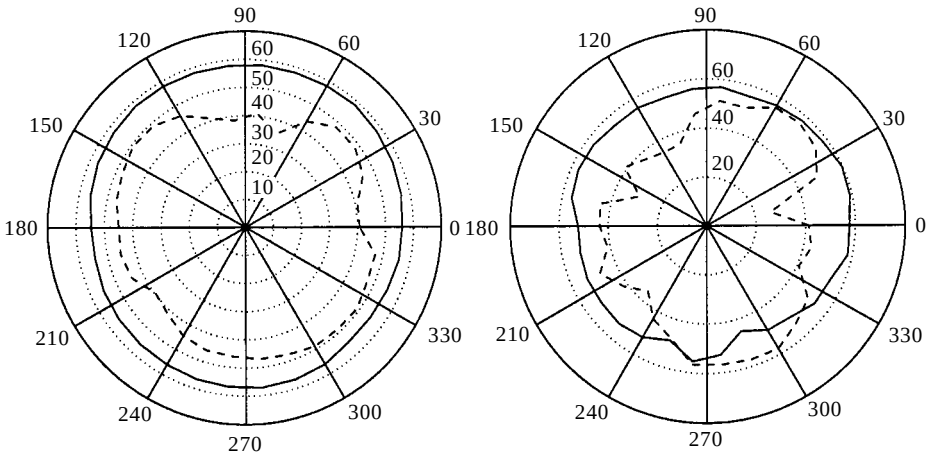

Figure 12. Sound pressure levels (dB) at $z = 0{\cdot}6$ m ($\theta = 13\pi/30$), without control (——), with control (—): (a) 100 Hz; (b) 200 Hz.

3.3. STRATEGY AND IMPOSED CONSTRAINTS

The number of secondary loudspeakers was limited to eight and the number of error sensors to 10 because of the capabilities of our electronic controller. The genetic algorithm allowed the selection of eight loudspeakers among 28. For error sensor selection, it was decided to select 10 microphone positions among the 60 lower positions in the planes $\theta = 13\pi/30$ ($z = 0{\cdot}6$ m) and $\theta = 11\pi/30$ ($z = 1{\cdot}2$ m) instead of the 210 positions. These microphone positions were chosen because the initial reduction with 210 error sensors was low (15 dB at 100 Hz and 9 dB at 200 Hz); thus, a selection of 10 sensor positions among 210 would not give good results. Of course, choosing the 60 lower positions precludes sound reduction in the higher positions. Nevertheless, a sound reduction in all directions

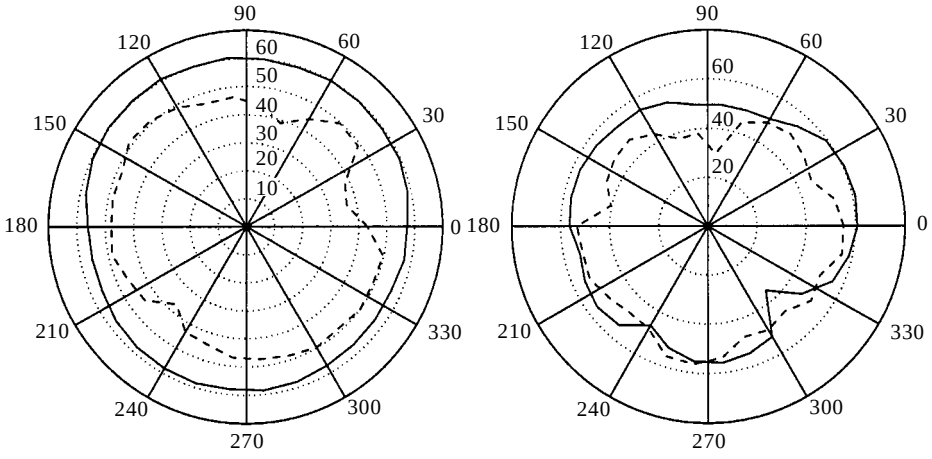

Figure 13. Sound pressure levels (dB) at $z = 1{\cdot}2$ m ($\theta = 11\pi/30$), without control (——), with control (—): (a) 100 Hz; (b) 200 Hz.

in the area $0 \leqslant z \leqslant 1{\cdot}2$ would lead to a marked acoustic shadow at long distances (12 m of height 30 m from the transformer).

3.4. NUMERICAL AND EXPERIMENTAL RESULTS

The parameters of the X-LMS algorithm were $F_c = 830$ Hz, $F_e = 412$ Hz, $N_h = N_w = 10$. A reference signal taken on the electric network was used. Figure 11 is a view from the top of the active control system. Table 4 compares the numerical and experimental values of the criterion GR computed with the 60 lower measurement points instead of the 210 of equation (3). Figure 12 shows the experimental sound pressure levels with and without control in the lower plane of microphones ($z = 0{\cdot}6$ m). Figure 13 is the same representation for the plane of microphones at $z = 1{\cdot}2$ m. On Figures 12 and 13, the sound pressure level at 100 Hz is reduced in all directions (from 10 to 25 dB) in both planes. At 200 Hz, the reduction is more irregular and reaches 30 dB in some directions, but an increase in sound level (from 5 to 10 dB) appears in a very limited area. In Table 4, the discrepancy observed between simulation and experiment is due to the fluctuations of the transformer radiation. In fact, the sound field radiated by the transformer depends on the voltage applied to the transformer, the temperature, and the phase variation of the coils. Thus, the configuration of actuators and error sensors established from a numerical simulation using one primary field is no longer optimal if this primary field is different for the experiment. Nevertheless, the real time active control is optimal because the X-LMS algorithm is adaptive.

4. CONCLUSION

Rather than the empirical approach commonly used, which consists of uniform distribution of actuators and sensors around the primary source, it was shown that a mixed method using a model of the primary field and selective search algorithms provides a solution near the optimal.

It was evidenced that it is possible to globally and significantly reduce the sound radiated by a small primary source by up to 300 Hz with two groups of three loudspeakers shifted from the primary source and seven error microphones located all around it. The adequacy between simulation and experimental results proves that the optimization is successful.

For an extended primary source like the transformer, in spite of the imposed constraints (few actuators and error sensors, imposed distance between the actuators and the transformer), it was shown that the sound level at 100 and 200 Hz could be reduced in all azimuthal directions in the area $0 \leqslant z \leqslant 1{\cdot}2$. Note that the previous studies on active noise control of transformer noise which gave equivalent results were obtained with dense arrays of loudspeakers and microphones [5]. The studies using simpler systems gave good results only in very limited areas [6–8].

Thus, the performances of our active control system with only eight loudspeakers and 10 error microphones are very promising for practical applications in an industrial situation. Finally, the results could be improved by reasonably increasing the number of loudspeakers and decreasing the distance between the loudspeakers and the transformer. The active system would be more efficient and would remain realistic for practical implementation.

Another advantage of the proposed method is that the configuration obtained in free space which reduces the field in all directions, could also be a good one in a bounded medium.

REFERENCES

1. T. Martin and A. Roure 1997 *Journal of Sound and Vibration* **201**, 577–593. Optimization of an active noise control system using spherical harmonics expansion of the primary field.
2. D. E. Goldberg 1989 *Genetic Algorithms in Search*, *Optimization and Machine Learning*. Reading, MA: Addison-Wesley Publishing Company.
3. K. H. Baek and S. J. Elliot 1995 *Journal of Sound and Vibration* **186**, 245–267. Natural algorithms for choosing source locations in active control systems.
4. D. A. Manolas, T. Gialamas and D. T. Tsahalis 1996 *Proceedings Internoise* '96, 1187–1191. A genetic algorithm for the simultaneous optimization of the sensor and actuator positions for an active noise and/or vibration control system.
5. S. E. Craig and O. L. Angevine 1993 *Proceedings of Second Conference on Recent Advances in Active Control of Sound and Vibration*, 279–290. Active control of hum from large power transformers—the real world.
6. W. B. Conover and R. J. Ringlee 1955 *Transactions of the AIEE Part III Power Apparatus and Systems* **74**, 77–90. Recent contributions to transformer audible noise control.
7. K. Kido and S. Onoda 1972 *Technical Report* 23, *Science Reports of the Research Institutes*, *Tohoku University* (*RITU*). Automatic control of acoustic noise emitted from power transformer by synthesizing directivity.
8. C. F. Ross 1978 *Journal of Sound and Vibration* **61**, 473–480. Experiments on the active control of transformer noise.